The Very Stable Boundary Layer on Nights with Weak Low-Level Jets

ROBERT M. BANTA
Chemical Sciences Division, Earth System Research Laboratory, National Oceanic and Atmospheric Administration, Boulder, Colorado

LARRY MAHRT AND DEAN VICKERS
College of Oceanic and Atmospheric Sciences, Oregon State University, Corvallis, Oregon

JIELUN SUN
National Center for Atmospheric Research, Boulder, Colorado

BEN B. BALSLEY
Cooperative Institute for Research in Environmental Sciences, University of Colorado, Boulder, Colorado

YELENA L. PICHUGINA AND ERIC J. WILLIAMS
Cooperative Institute for Research in Environmental Sciences, University of Colorado, and Chemical Sciences Division, Earth System Research Laboratory, National Oceanic and Atmospheric Administration, Boulder, Colorado

(Manuscript received 10 August 2006, in final form 6 December 2006)

ABSTRACT

The light-wind, clear-sky, very stable boundary layer (vSBL) is characterized by large values of bulk Richardson number. The light winds produce weak shear, turbulence, and mixing, and resulting strong temperature gradients near the surface. Here five nights with weak-wind, very stable boundary layers during the Cooperative Atmosphere–Surface Exchange Study (CASES-99) are investigated. Although the winds were light and variable near the surface, Doppler lidar profiles of wind speed often indicated persistent profile shapes and magnitudes for periods of an hour or more, sometimes exhibiting jetlike maxima. The near-surface structure of the boundary layer (BL) on the five nights all showed characteristics typical of the vSBL. These characteristics included a shallow traditional BL only 10–30 m deep with weak intermittent turbulence within the strong surface-based radiation inversion. Above this shallow BL sat a layer of very weak turbulence and negligible turbulent mixing. The focus of this paper is on the effects of this quiescent layer just above the shallow BL, and the impacts of this quiescent layer on turbulent transport and numerical modeling. High-frequency time series of temperature T on a 60-m tower showed that 1) the amplitudes of the T fluctuations were dramatically suppressed at levels above 30 m in contrast to the relatively larger intermittent T fluctuations in the shallow BL below, and 2) the temperature at 40- to 60-m height was nearly constant for several hours, indicating that the very cold air near the surface was not being mixed upward to those levels. The presence of this quiescent layer indicates that the atmosphere above the shallow BL was isolated and detached both from the surface and from the shallow BL.

Although some of the nights studied had modestly stronger winds and traveling disturbances (density currents, gravity waves, shear instabilities), these disturbances seemed to pass through the region without having much effect on either the SBL structure or on the atmosphere–surface decoupling. The decoupling suggests that under very stable conditions, the surface-layer lower boundary condition for numerical weather prediction models should act to decouple and isolate the surface from the atmosphere, for example, as a free-slip, thermally insulated layer.

A multiday time series of ozone from an air quality campaign in Tennessee, which exhibited nocturnal behavior typical of polluted air, showed the disappearance of ozone on weak low-level jets (LLJ) nights. This behavior is consistent with the two-stratum structure of the vSBL, and with the nearly complete isolation of the surface and the shallow BL from the rest of the atmosphere above, in contrast to cases with stronger LLJs, where such coupling was stronger.

Corresponding author address: Robert M. Banta, NOAA/CSD3, 325 Broadway, Boulder, CO 80305.
E-mail: robert.banta@noaa.gov

DOI: 10.1175/JAS4002.1

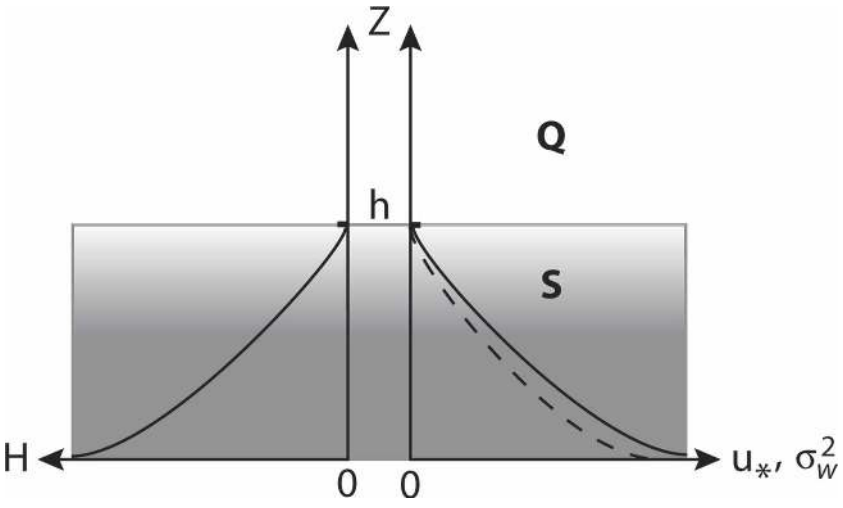

FIG. 1. Schematic profiles of heat flux H, vertical velocity variance σ_w^2, and friction velocity u_* showing traditional BL structure. Shaded portion marked S represents the shallow BL, and the region above marked Q represents the quiescent layer aloft.

1. Introduction

Turbulent transport and mixing processes near the earth's surface provide a major control over the rate of transfer between the surface and the free atmosphere of such quantities as momentum, heat, and airborne trace species. The ability to accurately determine turbulent transfer rates is an important goal for increasing basic understanding of surface–atmosphere exchange processes, as well as for improving their representation in numerical weather prediction (NWP) models. Further, since the surface acts as a source or sink of these quantities, near-surface interaction is a key component of these budgets.

In particular, recent research emphasis on the stable boundary layer (SBL) reflects the need to better understand these processes under stable conditions. Especially elusive and difficult is the very stable boundary layer (vSBL), characterized by Mahrt et al. (1998) as having weak winds, clear skies, and strong radiative cooling at the surface. Under vSBL conditions, the strong stability of the radiational temperature inversion is effective in suppressing both turbulence and turbulent mixing, thereby producing a vertically thin, highly structured BL, in which turbulent processes occur in intermittent bursts.

In the traditional, shear-driven BL the magnitudes of fluxes and other turbulence quantities averaged over some time or space scale have maximum values at the surface and decrease to near zero at the top, as shown in Fig. 1. Under very stable, weak-wind conditions, this structure has been found to occupy a very shallow layer—sometimes 10 or fewer meters deep—adjacent to the surface. In the present investigation, case-study data from the Cooperative Atmosphere–Surface Exchange Study campaign of October 1999 (CASES-99) show this shallow-BL structure. Here we present further analysis of this dataset, indicating a second region or layer just above this BL, in which turbulent mixing is strongly suppressed. This layer, which is important for applications, has not been described in previous SBL studies. Above these two layers turbulence may still be active at higher levels, sometimes associated with low-level jets (LLJs) when present.

Existing analyses of the CASES-99 dataset have emphasized the importance of shear-generated turbulence near the LLJ and coupling with the ground surface (e.g., Blumen et al. 2001; Poulos et al. 2002; Mahrt and Vickers 2002; Banta et al. 2002, 2003, 2006; Newsom and Banta 2003; Sun et al. 2002, 2004; Balsley et al. 2006, and others). On weak wind nights, however, such shear generation either does not exist or at least does not influence the surface-based boundary layer. The present study emphasizes these cases. The results reveal that the surface-based boundary layer becomes remarkably thin, and smaller than the vertical resolution of many NWP models. Turbulence in the overlying quiescent layer is extremely weak, so that the influence of surface fluxes is confined to a thin layer.

We investigate this typical structure on five nights of CASES-99, and we discuss implications of this structure for turbulent interaction between the surface and the atmosphere, for NWP parameterization of the surface layer, and for the nighttime behavior of the pollutant ozone. The five study nights are considered in order of increasing LLJ wind speeds. Nights with the weakest

speeds showed no interruptions of the basic vSBL structure. As LLJ speeds increased modestly, more frequent occurrences of disturbances, such as density currents, gravity waves, and shear instabilities, were noted. Improved understanding and modeling of the vSBL will depend on learning about whether and how these events influence the structure of mean profiles in the vSBL.

Improved understanding of SBL processes is needed for application in several areas, including representation of these processes in NWP models. At the lower boundary of a model, surface-layer fluxes are generally modeled using a stability function or stability-dependent drag coefficient that decreases from neutral flux values for weak stability to values that diminish as conditions become very stable (Beare et al. 2006; Steeneveld et al. 2007). In practice a lower limit, or slow decline with stability (long-tails function; Beare et al. 2006), is often imposed on the fluxes in the models so that fluxes cannot get too small. The justification cited for this limitation is the empirical notion that some turbulence is always present and that many atmospheric processes produce vertical transport or mixing at atmospheric scales that are subresolution in the model. Thus, presumably some background level of mixing is always present due to one mechanism or another. The advantage to the model is that the enhanced simulated mixing distributes cooling, for example, over deeper layers to prevent runaway cooling effects, which have been noted in simulations (Louis 1979; Derbyshire 1999; Poulos and Burns 2003).

In the present study, the focus will be on the existence and effects of the layer of weak turbulence and suppressed mixing just above the shallow BL. The next section (section 2) provides a review of pertinent literature on shallow BLs, the CASES-99 project, and the CASES-99 instrumentation used in this study. Section 3 presents observations of shallow BL structure and evidence for the existence of, and the effects of, the layer of suppressed turbulence just above the shallow BL. In section 4 we relate the nocturnal behavior of the pollutant ozone near the surface to the vSBL findings in section 3. We also discuss approaches to NWP modeling of the surface layer at the lower model boundary. The conclusions in section 5 include a brief summary of findings.

2. Background and measurements

Many studies have attempted to classify the SBL structure by stability (e.g., Mahrt 1985, 1999; Holtslag and Nieuwstadt 1986; Holtslag and De Bruin 1988; Mahrt et al. 1998; Derbyshire 1999; Ohya 2001; Van de Wiel et al. 2002, 2003; Grachev et al. 2005). Definitions of stability regimes have involved both surface-layer and local forms of the Monin–Obukhov length L. Correlations between the nondimensional wind shear and z/L are often dominated by spurious self correlations, which prevent physical conclusions and reduce the utility of z/L as a stability parameter (Klipp and Mahrt 2004; Baas et al. 2006). The gradient Richardson number can be vulnerable to errors in estimating local vertical gradients. Mahrt and Vickers (2006) argued that the turbulence even near the surface is related to bulk Richardson number over a deep layer,

$$\mathrm{Ri_B} = g\left(\frac{\Delta\theta}{\Delta z}\right) \Big/ \theta\left(\frac{\Delta U}{\Delta z}\right)^2.$$

Here θ is potential temperature, U the mean wind, z the height above the surface, Δ represents differences across the layer depth over which $\mathrm{Ri_B}$ is evaluated, and g is the acceleration of gravity. Banta et al. (2003) defined a jet Richardson number $\mathrm{Ri_J}$, in which the shear was estimated from the speed U_X and height Z_X of the first LLJ wind-speed maximum above the surface,

$$\mathrm{Ri_J} = g\left(\frac{\Delta\theta}{\Delta z}\right) \Big/ \theta\left(\frac{U_x}{Z_x}\right)^2.$$

Mean wind and θ often tend to vary nearly linearly with height in the layer between the surface layer and Z_X (Banta et al. 2003, 2005), so that $\mathrm{Ri_B}$ and $\mathrm{Ri_J}$ are often nearly interchangeable, except that sometimes uncertainties in determining Z_X from data can lead to slight overestimates of $\mathrm{Ri_J}$. A plot of turbulence kinetic energy (TKE) measured in the subjet layer against either value of Ri (e.g., Fig. 2) shows that the regime of the very stable BL (indicated as S on Fig. 2) is marked by small values of TKE when either Ri exceeds about 0.3, although the sample size does not permit a specific critical value of the Richardson number to be identified (0.25 is well within the range of uncertainty).

The major defining property of the vSBL is weak winds, resulting from slack pressure gradients often associated with anticyclonic conditions and clear skies. In the SBL classification scheme recently developed by Van de Wiel (2002, 2003), which is based on a large-scale pressure gradient and the net surface radiation, the vSBL is referred to as the radiation SBL, reflecting the lack of influence of wind-related processes. Weak winds generate weak shears, and weak turbulence and mixing, which allow the buildup of cold air near the surface, resulting in increased static stability.

Difficulties in obtaining consistent characterizations of the vSBL are a consequence of the weak and intermittent turbulence, because the stratification of the

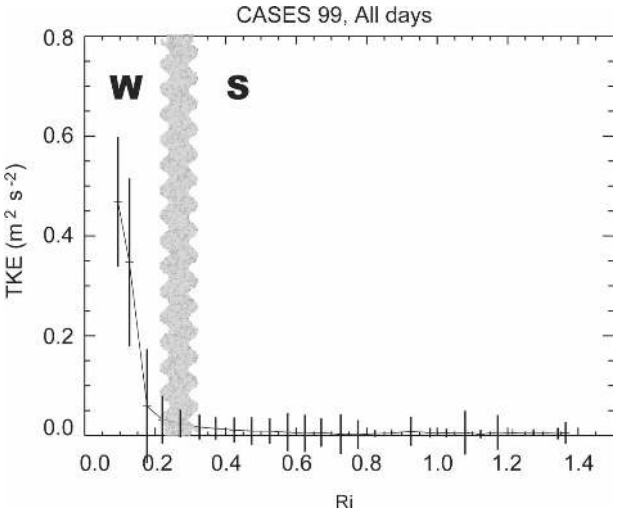

FIG. 2. Plot of TKE vs bulk Richardson number Ri for all nights of CASES-99 from Banta et al. (2003). TKE data were divided into bins of width 0.05 based on Ri values, and solid line connects the median of TKE values in each bin. Error bars indicate ± one standard deviation of TKE values in each bin. W indicates approximate region of weakly stable BL, and S, the region of the strongly stable BL.

vSBL supports disturbances other than turbulence that do not mix out. These disturbances, which Mahrt and Vickers (2006) refer to as mesoscale motions, sporadically perform vertical transport and exchange at magnitudes that can overwhelm the diffusive contributions of the purely turbulent fluxes. Examples may include packets of Kelvin–Helmholtz instabilities, propagating gravity waves, density currents, solitary waves, and topographically induced w patterns. Such topographic w patterns can arise from the effects of drainage flows, which can form over even gently sloping cool surfaces. These flows are common in weak-wind, clear-sky conditions, so that they can be considered characteristic of the vSBL (Mahrt et al. 2001; Soler et al. 2002). In addition to producing weak mixing from shear instability, drainage flows also produce localized divergence patterns, because of the horizontal variability of the topography. The divergence patterns produce the localized w patterns. Although thin and weak, the potential impact of drainage flows is that they can generate localized vertical transport that is significant compared to the background mixing that would occur without drainage flows.

a. Shallow vSBL studies

The present study builds on two previous studies of the weak-wind vSBL, Smedman (1988) and Mahrt and Vickers (2006), both of which found shallow BLs less than a few tens of meters deep during very stable conditions. Smedman (1988) investigated SBL structure for two consecutive February nights using an instrumented 30-m tower and a sodar over a flat, snow-covered site in southern Sweden. Vertical profiles of gradient Ri indicated SBL depths consistently less than 10 m for most of both nights, and SBL depths calculated from the Zilitinkevich (1972) formula, $h_t = c(Lu_*/f)^{1/2}$, where u_* is the fraction velocity, were generally 10–30 m (in this formula h_t is the depth of the turbulent SBL, f the Coriolis parameter, and $c = 0.4$). The magnitude of the tower-measured turbulence was tabulated over the two nights for nineteen 60-min-averaging periods or runs. The median values of σ_w^2 and kinematic heat flux H in the shallow BL at 2-m height were 0.005 $m^2 s^{-2}$ and -0.003 K $m s^{-1}$, respectively, for the 19 runs.

The development of appropriate analysis procedures to separate the effect of purely turbulent processes from the other features or disturbances, such as those described above, in producing vertical exchange, was an important step in understanding turbulent mixing processes in the vSBL. The other disturbances (or "mesoscale motions" of Mahrt and Vickers 2006) occur routinely at lower frequency than turbulence, especially in the vSBL. Such fluxes can be upward or downward and show no relation to the local profiles. Thus it is probably necessary to consider the lower-frequency disturbances separately from turbulence in analyzing datasets and in formulating models or parameterizations of vSBL processes.

Vickers and Mahrt (2006) addressed this problem by defining variable averaging windows for determining perturbations, where the window widths change from record to record according to the cospectral-gap frequency at that time. For reference, this variable record length, which averaged about 30 s, could range from 10 to >100 s. Fluxes from these shorter windows were then averaged over a longer interval, to reduce the randomness inherent in turbulence and achieve statistical significance. For the present study, this longer interval was chosen to be 1 h. Fluxes and other turbulent quantities calculated using this multiresolution flux decomposition approach were found to be well behaved, in the sense of smoothly varying cospectra, heat fluxes consistently downgradient, and smooth interval-to-interval variation of turbulence quantities (Vickers and Mahrt 2006; Acevedo et al. 2006; Van den Kroonenberg and Bange 2007). This behavior is an indication that the procedure successfully isolates purely turbulent effects from the lower-frequency motions.

This method for calculation of turbulence with variable window widths was used in the second study of extremely stable boundary layers, the study by Mahrt

and Vickers (2006), in which data from three field campaigns, processed in this way, were composited to characterize the turbulence structure of vSBLs. The dataset consisted of nearly 1000 h of turbulence profile data from the three projects. Profiles of σ_w^2 and fluxes for the composites of hours with weak turbulence exhibited a traditional BL structure, in agreement with Smedman (1988), with depths of 5–25 m. Typical magnitudes of σ_w^2 and kinematic heat flux H in the shallow BL at 2- or 5-m height were 0.0010 $m^2 s^{-2}$ and 0.0005 K $m s^{-1}$, respectively. That these values were somewhat smaller than those of Smedman (1988) may be due in part to location or seasonal differences.

Mahrt and Vickers (2006) demonstrated using turbulent time series of w that the quiet periods are also turbulent, but with much-reduced amplitudes of fluctuation, providing evidence for the notion that some turbulence is always present in the atmosphere, even if very weak. It is important to note, however, that the amplitudes of the turbulent variances and fluxes are orders of magnitude weaker during the quiet periods, and thus vertical mixing during these periods is essentially nonexistent over time periods of several hours or a night. In particular, the presence of this very weak turbulence is not to be construed as justification for using the relatively high background turbulence or mixing levels often found in current NWP models. Mahrt and Vickers also found that layer or bulk Ri is the appropriate measure of stability, as opposed to z/L (owing to the self-correlation problem, as previously noted), and they found evidence of enhanced horizontal advective effects for a site with greater horizontal topographic variability than the others. Effects resulting from horizontal inhomogeneities, which may not appear strongly under unstable-convective or even weakly stable conditions, can have a noticeable effect on weak nocturnal turbulent processes in the vSBL.

b. Instrumentation

CASES-99 was a monthlong field campaign over the grassland of southeastern Kansas designed to study the nocturnal SBL (Poulos et al. 2002). The main site, south of Leon, Kansas, had in situ and remote sensing instrumentation used in the present study, which included sensors mounted on the main, 60-m-tall, scaffolding tower, the kite- or balloon-borne tethered lifting system (TLS), and the high-resolution doppler lidar (HRDL). The official project time standard for CASES-99 was the coordinated universal time (UTC), which is 6 h ahead of local standard time; sunset was just before 0000 UTC, and local midnight was at 0600 UTC.

Tower instrumentation at the main site has been described by Sun et al. (2003) and Poulos et al. (2002). It consisted of eight levels of sonic anemometers and other eddy-correlation sensors, 34 levels of thermocouples, four levels of propeller–anemometer and wind-vane sensors, and six levels of aspirated thermistor data. Fluxes were calculated using 20-Hz velocity and virtual-temperature measurements collected by sonic anemometers located at six levels (10, 20, 30, 40, 50, and 55 m) on the main 60-m tower and two levels (1.5 and 5 m) on a shorter tower located 10 m away from the main tower. The high-frequency data were analyzed using the multiresolution flux decomposition procedures (Vickers and Mahrt 1997, 2003, 2006; Acevedo et al. 2006; Van den Kroonenberg and Bange 2006) described earlier in this section, to produce hourly profiles of σ_w^2, momentum flux, and heat flux. Temperature (T) data were also obtained at 5 Hz by 34 thermocouples mounted at vertical intervals of 1.8 m between 2.3 and 58.1 m on the main tower. Data characteristics and analysis procedures are described by Burns and Sun (2000), Poulos et al. (2002), and Sun et al. (2002).

Vertical profiles of TKE dissipation ε were measured at the main site by ascents and descents of the TLS, built and deployed by the Cooperative Institute for Research in Environmental Sciences (CIRES). The TLS employs either an aerodynamic balloon (for light-wind conditions) or a kite (for moderate to strong wind conditions) to lift lightweight packages of instrumentation up to 2 km above ground to measure mean and turbulent atmospheric variables (Balsley et al.1998, 2003, 2006; Frehlich et al. 2003; Muschinski et al. 2004). A basic meteorological payload measures atmospheric temperature, pressure, humidity, and wind speed and direction at 1 Hz. Up to five turbulence packages separated vertically at selected intervals (often ~5 m) can be attached either above or below the basic package, using cold- and hot-wire sensors to provide high-frequency temperature and wind-speed measurements at 200 Hz. From the high-frequency wind-fluctuation measurements, ε values can be calculated as a function of height, following the procedures described in Balsley et al. (2003, 2006). For the present study, TLS ascents were only available for three of the five study nights (14, 18, and 20 October), and the results for 14 October are presented in Balsley et al. (2006).

The HRDL scanned from a site 1.2 km to the south of the main tower site (Newsom and Banta 2003; Poulos et al. 2002; Banta et al. 2002). HRDL's measurement precision is better than ~20 cm s^{-1}, and range resolution is 30 m. Other characteristics of the lidar system have been described by Grund et al. (2001) and Wulfmeyer et al. (2000), and its uses during CASES-99, by

TABLE 1. Mean LLJ properties and stability measures for 7 nights of CASES-99. Turbulence variables were measured at a height of 5 m.

	U_X m s^{-1}	$\partial\theta/\partial z$ K m^{-1}	$\mathrm{Ri_B}$	$\mathrm{Ri_J}$	L (m)	h_t (m)	h_s (m)	σ_w^2 m^2 s^{-2}	u_*^2 m^2 s^{-2}	H_0 K m s^{-1}	Time period
26 Oct[a]	3	>0.15	>2.0	>3.0	0.5	4	8	0.0016	<0.0004	−0.0008	0300–0700 UTC
20 Oct[a]	4	0.15	>2.0	>2.0	3.2	18	19	0.0065	0.0036	−0.0037	0300–0500 UTC
18 Oct	7	0.12	0.4	0.5	4.8	24	21	0.0088	0.0043	−0.0034	0300–1100 UTC
6 Oct	9	0.11	0.25[b]	0.6[b]	4.5	26	34	0.0119	0.0072	−0.0076	0200–0500 UTC
14 Oct	12	0.08	0.25	0.4	5.1	28	36	0.0122	0.0071	−0.0054	0300–0700 UTC
27 Oct	18[c]	0.07	0.15	0.2	17.0	77	88	0.0600	0.0378	−0.0259	0300–0700 UTC
25 Oct	19[c]	0.05	0.1	0.2	34.3	134	112	>0.1073	0.0656	−0.0255	0300–1100 UTC

[a] Prior to airmass change.
[b] Before midnight.
[c] After midnight.

Banta et al. (2002, 2006), Sun et al. (2002, 2004), Poulos et al. (2002), Newsom and Banta (2003), and Blumen et al. (2001). This study uses data from sequential vertical-slice scans (each taking ~30 s to complete) analyzed by procedures outlined in Banta et al. (2002, 2006). LLJ wind speed U_X and height Z_X were determined from a modified velocity–azimuth–display procedure also described in Banta et al. (2002), and values from the individual scans were averaged over 10 min.

Measurements of ozone O_3 were from another field experiment, the Southern Oxidants Study 1999 (SOS-99) summertime campaign in Nashville, Tennessee; O_3 was measured by a commercial ultraviolet absorption instrument (Model 49C; Thermo Environmental Instruments, Inc.). Nitric oxide NO was measured by a custom instrument via its chemiluminescence reaction with added O_3 (Thornton et al. 2003).

3. Observed structure

Data used for the five nights of this study are shown as the top five entries of Table 1. For contrast, the bottom two entries are data from the two strong-wind nights from CASES-99 that were used in the weakly stable BL study of Banta et al. (2006). The nights are arranged in order of increasing mean LLJ speed U_X, averaged over the period analyzed for each night. Included are estimates of BL height using formulae of Zilitinkevich (1972) and Steeneveld et al. (2007) [$h_s = 32\,(g\,|H_0|/\theta N^3)^{1/2}$], which are comparable for this small sample.

a. Mean wind vertical structure

The most important characteristic of the vSBL is low wind speeds in the lowest 100–200 m above the surface. Light winds are often thought to be associated with significant variability in speed and direction. Under such conditions it is not clear whether it makes sense to consider LLJ properties. To address this, Fig. 3 shows 10-min mean profiles of the wind speed in the lowest 300 m for the two weakest-wind study nights. Under the slack pressure-gradient conditions on these nights, the near-surface flow often was light and variable, and the profiles do show some periods of light, changeable winds. But they also show extended periods when the entire vertical structure remained nearly unchanged for periods of an hour or so. Such persistent structures include both profiles with no maximum and clear jetlike profiles that were apparent in many successive profiles. For example the profiles after 0300 and 0420 UTC do not exhibit a clear maximum, and those around 0700 and between 0520 and 0610 UTC 26 October (Fig. 3a) do have jetlike maxima. A similar plot on 20 October exhibits the same behavior (Fig. 3b). Thus, even under slack pressure-gradient and light-wind conditions, mean wind profiles within the lowest 300 m can contain periods of persistent structure, and can show LLJ structure for extended periods of time. Therefore, it is possible to define a maximum in the wind profile during these periods.

Time series of the speeds U_X and heights Z_X of LLJ maxima, derived from HRDL scan data from the five nights of this study, are shown in Fig. 4. LLJ speeds were less than 10 m s^{-1} on four of the nights and were relatively steady throughout the nights, remaining constant or changing slowly, except for late-night increases in wind speed on 26 and 20 October. These significant increases in wind speed occurred after 0830 UTC on 26 October and after 0630 UTC 20 October, as a result of weak synoptic-cold-front and density-current passages, respectively.

b. The vSBL structure during weak LLJ nights

Figure 4 shows LLJ speeds of only 2–3 and 4 m s^{-1} on 26 and 20 October, respectively, following the evening transition period during the first 2–3 h after sunset,

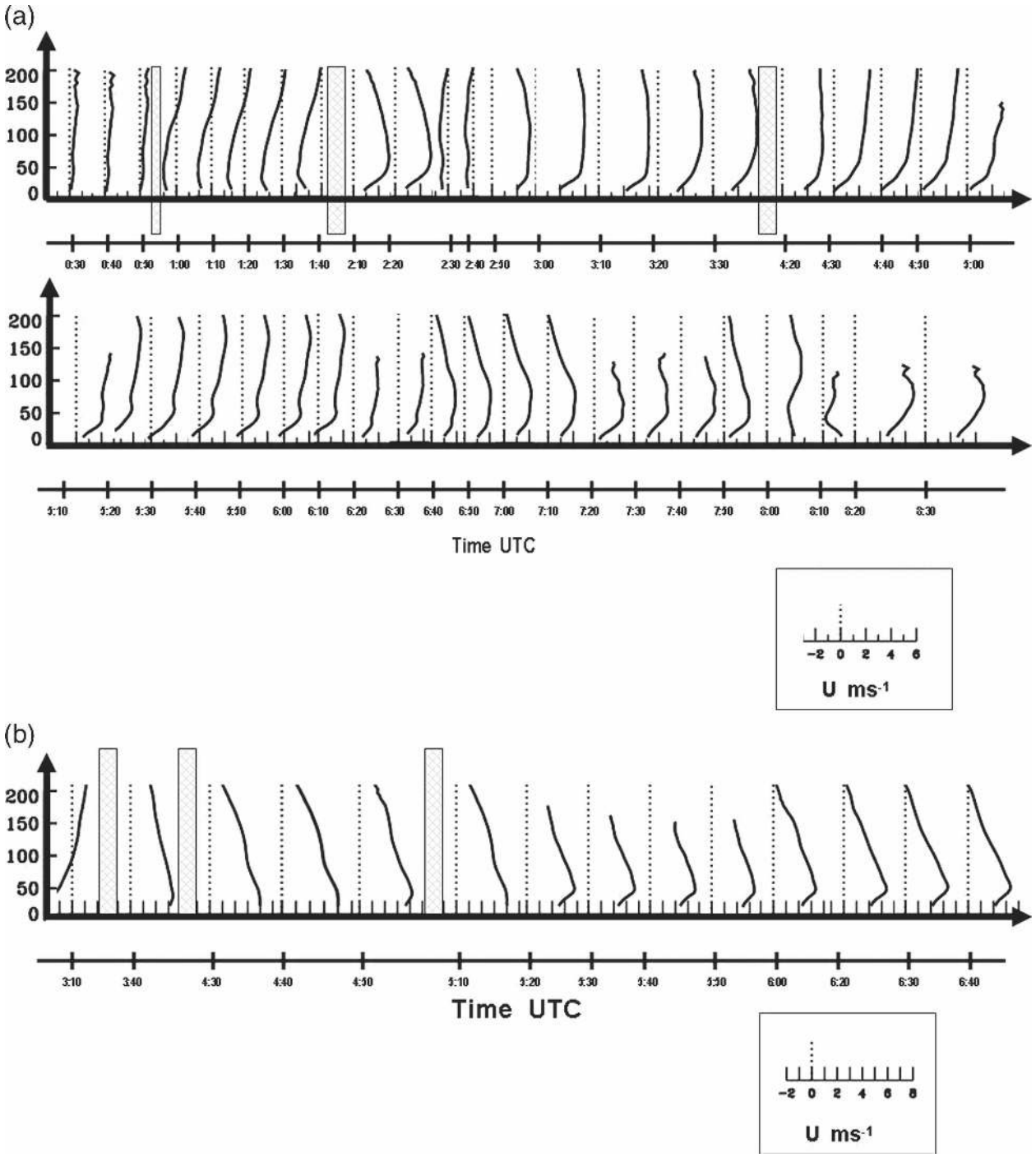

FIG. 3. Mean-wind profiles for (a) 26 Oct and (b) 20 Oct, averaged over 10 min, calculated from sequential vertical-slice scan data from HRDL, as described in Banta et al. (2002, 2006).

representing the smallest wind-speed maxima lasting more than 3 h during CASES-99. In this analysis, we consider only the periods on these two nights, when light winds were prevalent for several hours in the middle of each night, that is, after the 2–3 h evening transition but before the late-night airmass change and accompanying wind-speed increase. These were the most typical extended vSBL periods of the CASES-99 dataset. The Ri_B and Ri_J values calculated across the tower were >2 during the weak-wind periods (Table I).

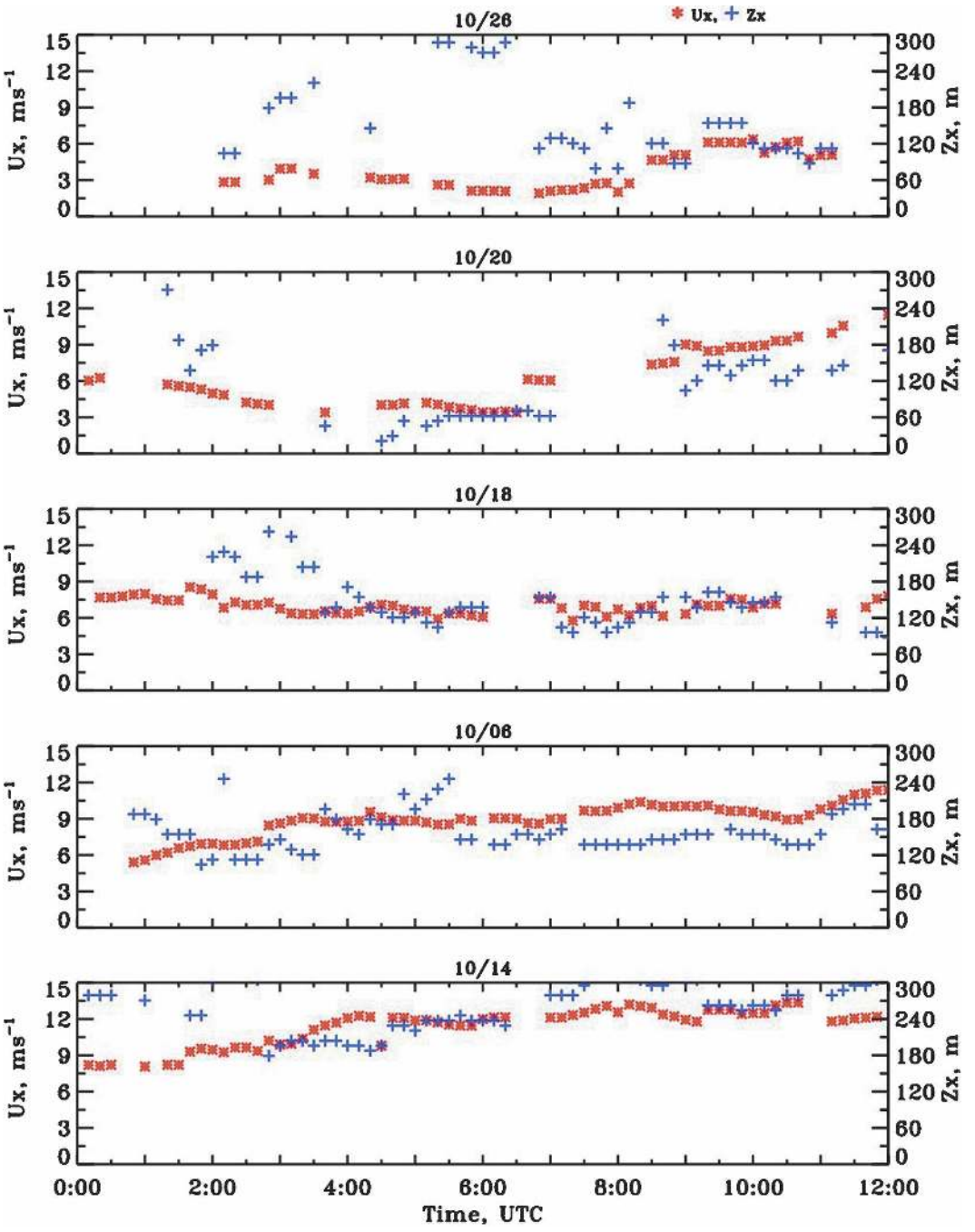

FIG. 4. Time series of U_X (red *, m s^{-1}, scale at left), and height of LLJ maximum Z_X (blue +, m, scale at right) for each weak LLJ night of this study, plotted as a function of hour UTC. Data were calculated from HRDL vertical-slice and conical data and averaged over 10-min intervals as described in Banta et al. (2002). Values were calculated from profiles using automated routines and then further checked visually; note that for some time intervals no maximum could be defined.

On 26 October the strong stability (Ri's often >10) produced very weak turbulence; for example TKE values of <0.05 m^2 s^{-2} were measured on the 60-m tower (see Fig. 5 of Banta et al. 2003). Our Fig. 5 presents time–height cross sections of tower data for 26 October. Several turbulence variables are shown, including vertical-velocity w variance σ_w^2 (top), friction-velocity u_* (middle), and heat-flux H (bottom) data. For most of

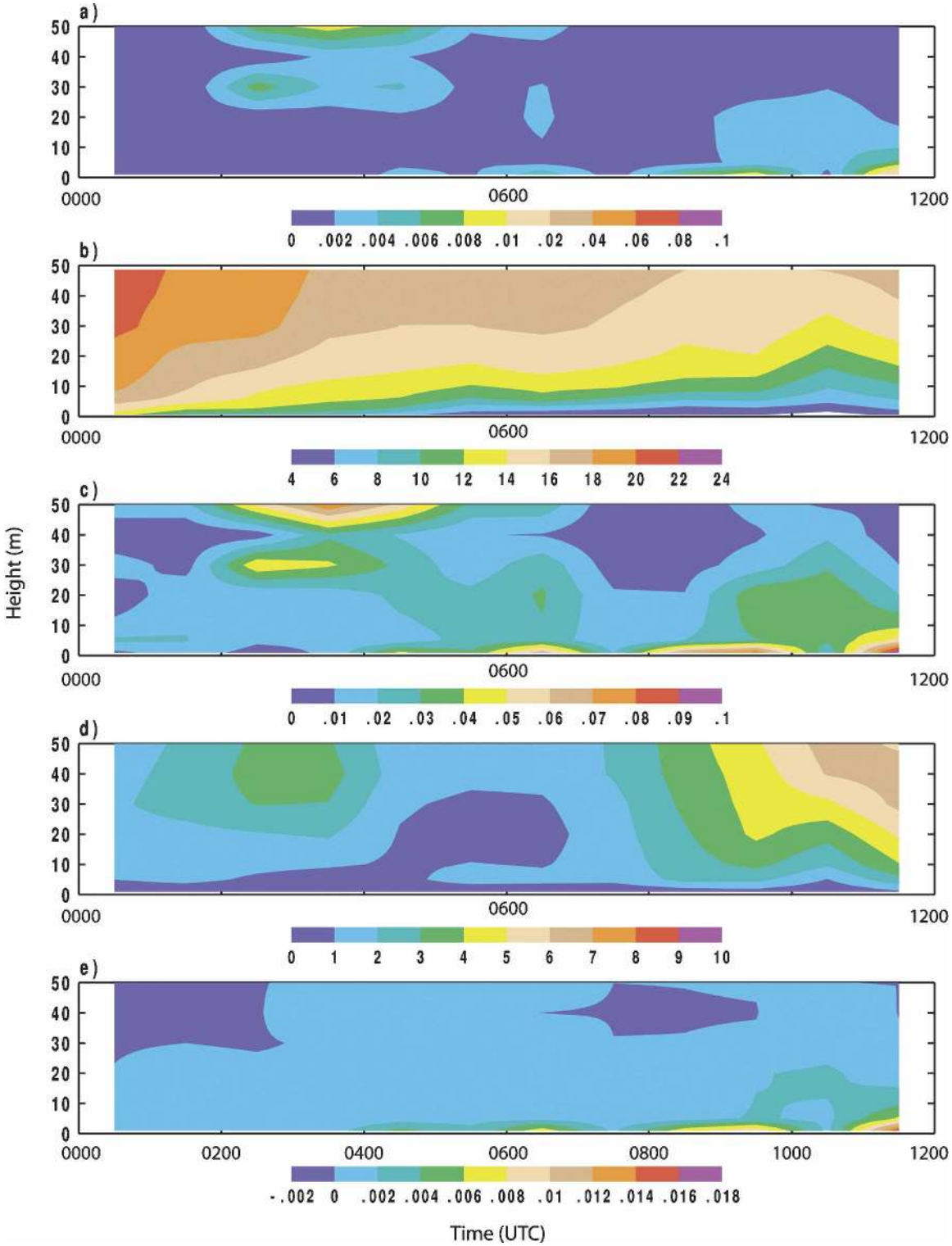

FIG. 5. Time–height cross sections of (a) w variance σ_w^2 ($m^2\,s^{-2}$), (b) temperature T (°C), (c) friction velocity u_* ($m\,s^{-1}$), (d) mean wind speed U ($m\,s^{-1}$), and (e) kinematic heat flux H ($K\,m\,s^{-1}$), for an example of a weak-LLJ night, 26 Oct 1999. Values were calculated from 60-m tower data.

the nighttime hours above the lowest few meters, the magnitudes of σ_w^2 across the 60-m tower were typically less than 0.004 $m^2 s^{-2}$; u_*, less than 0.02 m s^{-1}; and H, less than 0.002 K m s^{-1}. Values at 5-m height were even smaller, as recorded in Table 1. The weakness of the turbulent fluctuations can be appreciated by contrasting the values with those from 25 and 27 October (Table 1), which were two orders of magnitude greater. On 20 October, turbulence magnitudes were also very small in the tower time–height cross sections for all turbulence variables, although only σ_w^2 is shown (Fig. 6b). Significant turbulence events were mostly absent during most of both nights, especially above 10 m (Figs. 6a,b).

These nights show evidence of a very thin surface-based boundary layer, less than 10 m deep and not always well resolved by the data, and an overlying quiescent layer. In addition, the cross sections occasionally show evidence of turbulence activity above the quiescent layer at the top of the tower. Presumably, such turbulence can at times occur completely above the tower.

Vertical profiles of u_* and H during the period between the evening transition and the late-night wind-speed increases are given in Fig. 7. These profiles exhibit a stratified structure, consisting of 1) a weak traditional BL reaching as high as 30 m, but often less than 10 m, AGL, and 2) a region just above this shallow BL, where the turbulent fluxes became very weak. In the region aloft, values of u_* have decreased with height to less than 0.025 m s^{-1} and H, to less than 0.001 K m s^{-1}; H declined with height to consistently small values in this quiescent layer, but u_* often showed more variable behavior there, as seen by comparing Figs. 7a,c. The two-stratum structure was also very clear in TLS profiles of TKE dissipation ε from 20 October (Figs. 8a,b). These profiles show a drop of nearly two orders of magnitude from the shallow BL, where ε values were small at 10^{-4} $m^2 s^{-3}$, upward into the quiescent layer, where ε fell to very small values at 10^{-6} $m^2 s^{-3}$, indicating very weak turbulence (Balsley et al. 2006). Turbulence is also sometimes found above 70 m apparently generated by shear associated with the low-level jet. This behavior suggests that the tower will at least occasionally miss elevated turbulent events.

Tower T data give further insight into mixing effects in the quiescent region aloft. The time-height cross sections of T for the two nights (such as that in Fig. 5, second panel) show near-surface cooling after the evening transition but little change at the upper levels. Thermocouple temperature time series $T(t)$ at six levels (Figs. 9a,b) reinforce these findings, that T at the highest tower levels changed very little for several hours in the middle of each night (i.e., after the 3-h transitional period, but prior to the wind-speed increases associated with the airmass change). The constancy of T at the upper tower levels on both nights demonstrates that the much colder air near the surface was not being mixed upward to these levels [during CASES-99 cooling by radiative flux divergence was found to become weak after the first 3 h after sunset for the rest of the night (Sun et al. 2003)]. The finescale fluctuations measured at the highest levels of the tower were also suppressed, especially as compared with the lowest levels. This reduction of T fine structure is a further indication of the lack of turbulence at the upper levels, although weaker stratification aloft may also play a role.

Tower and TLS profile data thus show that, on the two nights with the weakest winds during CASES-99, the lowest two strata of the vSBL were the shallow BL next to the surface and a quiescent layer of negligible turbulent transport just above. At even higher levels, fleeting bursts of enhanced turbulent activity were occasionally evident in the CASES tower and TLS data (e.g., Figs. 7a, 8a,b). The bursts were still very weak (as distinct from the *extremely* weak background turbulence). In this upper region—as in the quiescent layer below—the relative constancy of $T(t)$ as well as the weakness of T fluctuations suggests a lack of mixing, which is another indication that the occasional weak, sporadic turbulence noted above the shallow BL was ineffective in producing any significant vertical stirring of the atmosphere between the surface and levels above the shallow BL.

c. Other nights

For comparison, we now examine nights with somewhat stronger winds. Three other nights exhibited weak turbulence in the tower layer, LLJ speeds generally less than 10 m s^{-1}, and shallow, weak, shear-driven BLs at the surface, and also provided complete tower and HRDL datasets. On these nights other structures or flow features were part of the nighttime evolution, including shear-flow instability events, density currents, and elevated inversion layers. We investigate the nature and impact of these disturbances or interruptions of the basic quiescent state on vertical mixing and on the development of SBL structure through the night.

1) TWO-STRATUM STRUCTURE

(i) 18 October

At 6–7 m s^{-1}, the LLJ speed on 18 October was somewhat stronger than on the two nights just considered, as shown on Fig. 4, and bulk Ri's were gen-

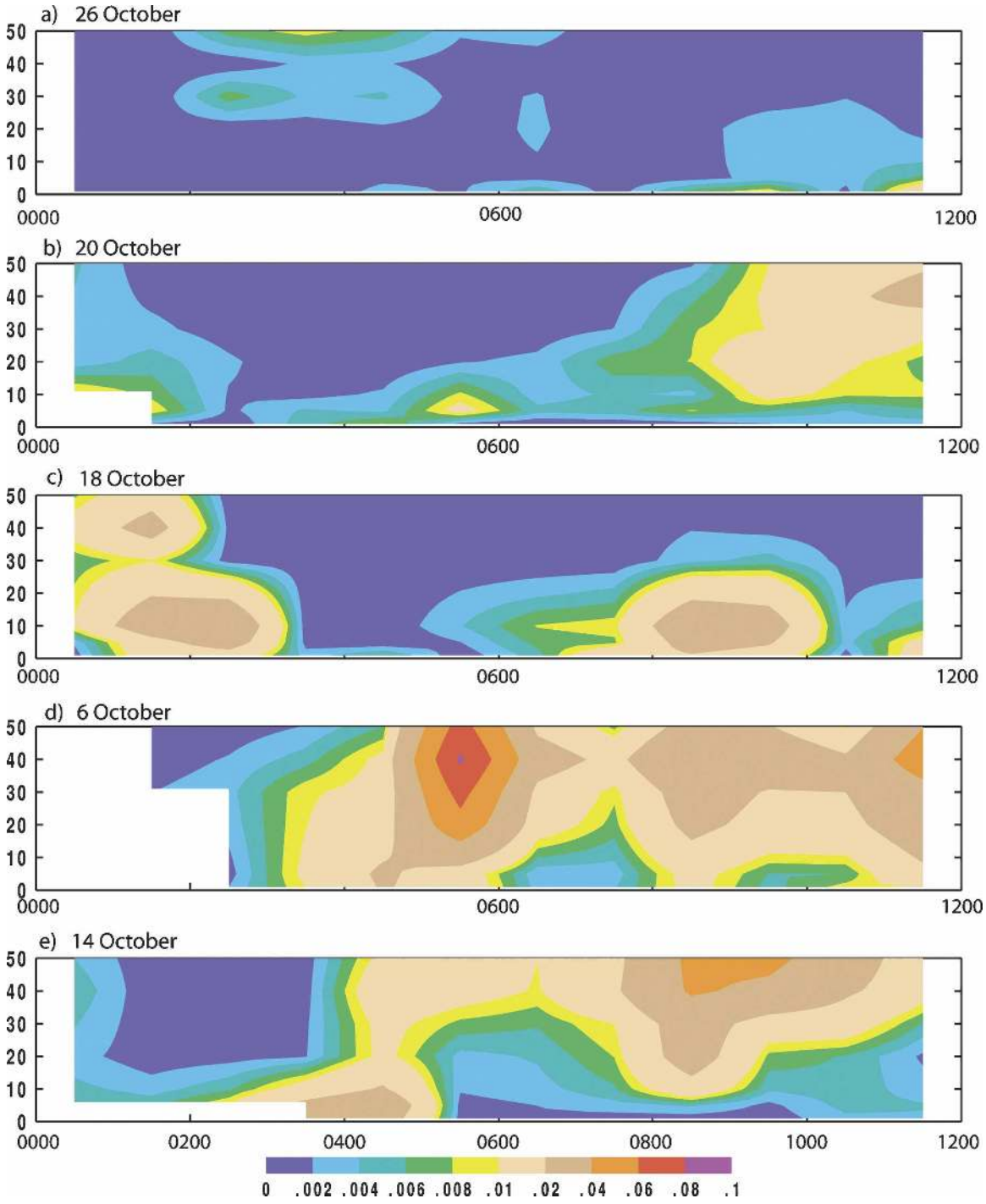

FIG. 6. Time–height cross sections of σ_w^2 for (a) 26 Oct (same as Fig. 5, top), (b) 20 Oct, (c) 18 Oct, (d) 6 Oct, and (e) 14 Oct. Time (horizontal axis) is in UTC, and height (vertical axis) is in meters above ground.

erally 0.5 to 0.8, becoming 0.3 to 0.5 after 0700 UTC. Figures 10a,b shows vertical profiles of u_* and H. These tower profiles, as well as the TLS ε profiles (Figs. 8c,d), reveal a shallow, weak BL with a quiescent layer just above, as in the previous two very stable cases. As further evidence of this structure, Sun et al. (2002) have provided time series of fluctuating w and T data from the 60-m tower (see Figs. 2 and 3 of that paper). These time series show intermittent periods of strong fluctuations at levels below 20–30 m, but much smaller ampli-

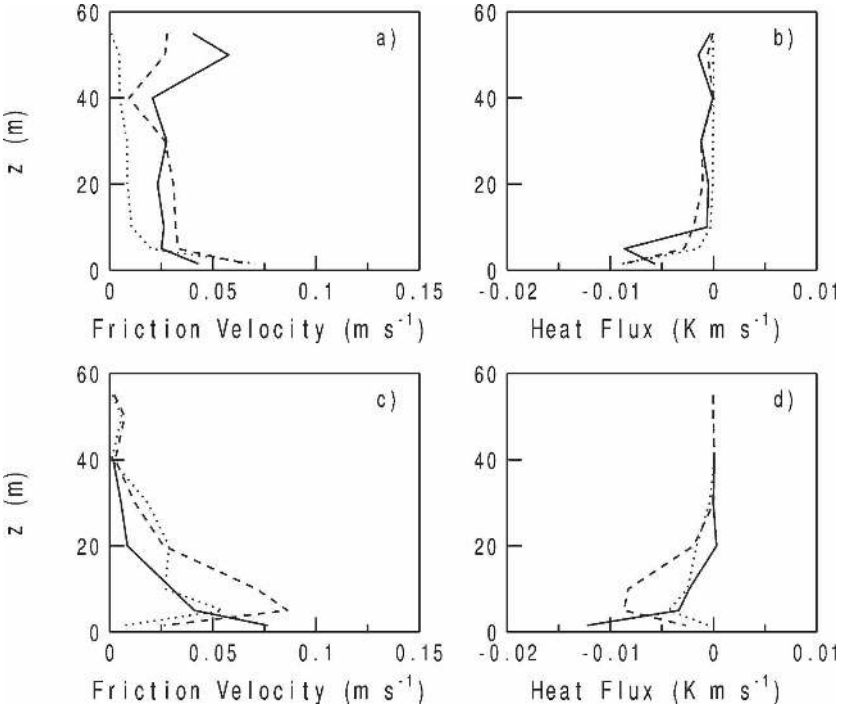

FIG. 7. Profiles of 60-min averaged u_* and H, averaged according to the Vickers and Mahrt (2006) procedure, showing traditional BL structure beneath quiescent layer for hours beginning 0400, 0600, and 0800 UTC (2200, 0000, and 0200 CST) (solid, dashed, dotted) on (a), (b) 26 Oct, and for (c), (d) hours beginning 0400, 0500, and 0600 UTC (2200, 2300, and 0000 CST) on 20 Oct.

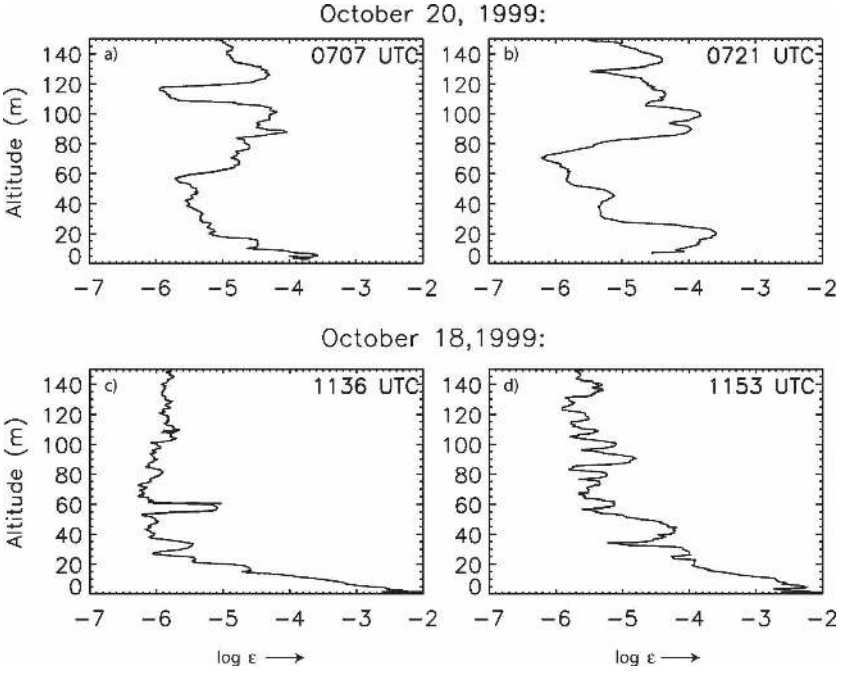

FIG. 8. Vertical profiles of logarithm of TKE dissipation ε, where ε is in $m^2 s^{-3}$, calculated from high-frequency (200 Hz) TLS data from (a), (b) 20 Oct 1999 and from (c), (d) 18 Oct 1999.

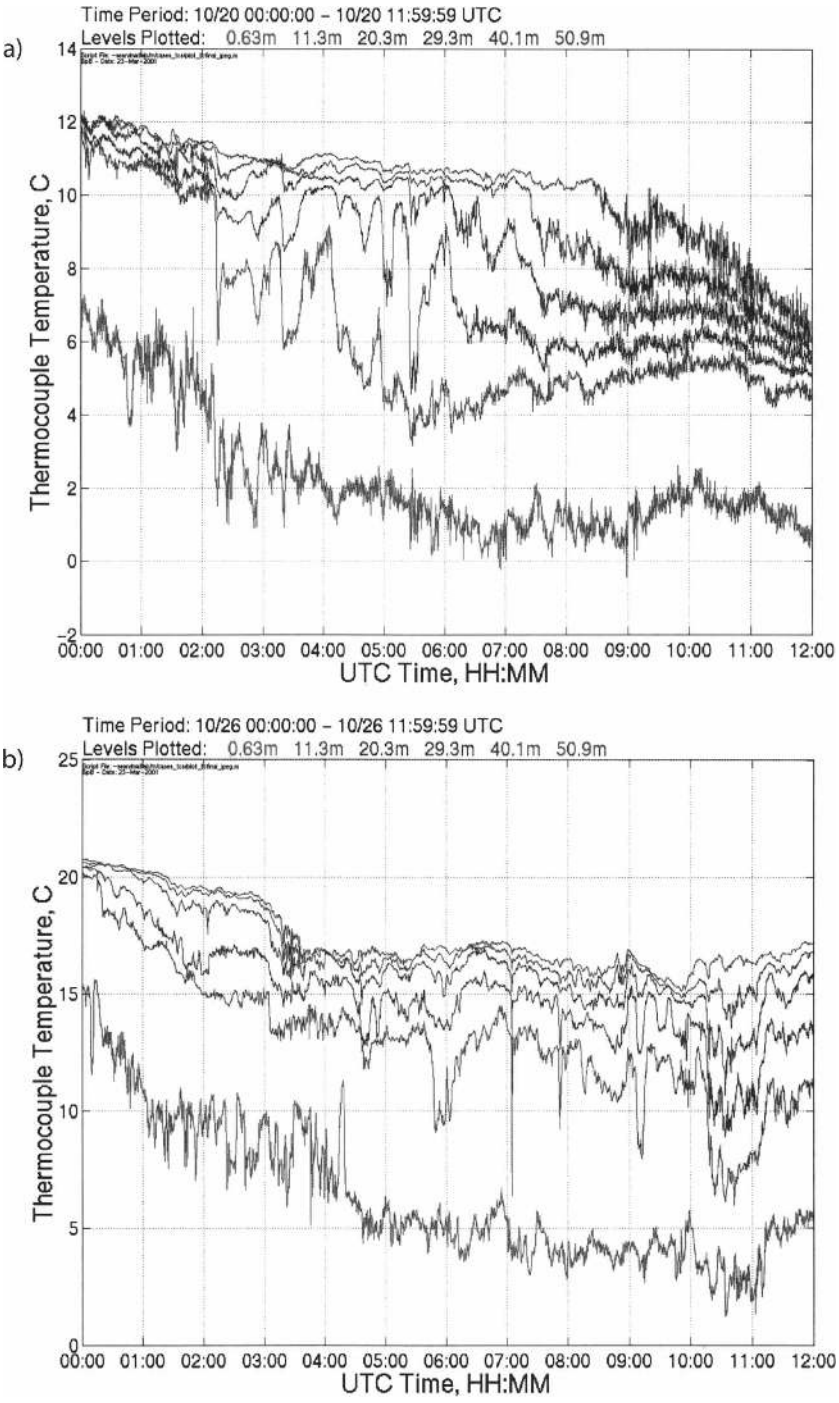

FIG. 9. Thermocouple time series (T; °C, obtained at 5 Hz) at six levels for (a) 26 Oct and (b) 20 Oct. On 20 Oct, the significant cooling at the upper tower levels starting at ~0800 UTC (and very evident after 0930 UTC) was a result of the airmass change and increased wind speeds.

tude turbulence at the upper levels (40, 50, 55 m) of the tower; that is, high-frequency fluctuations were considerably suppressed at the highest tower levels, as compared with the lower level, just as in the two previous cases. Thus, despite stronger shear than the two weak-wind cases of the previous section, the vertical structure of the turbulence was similar, providing another example of the two-stratum structure.

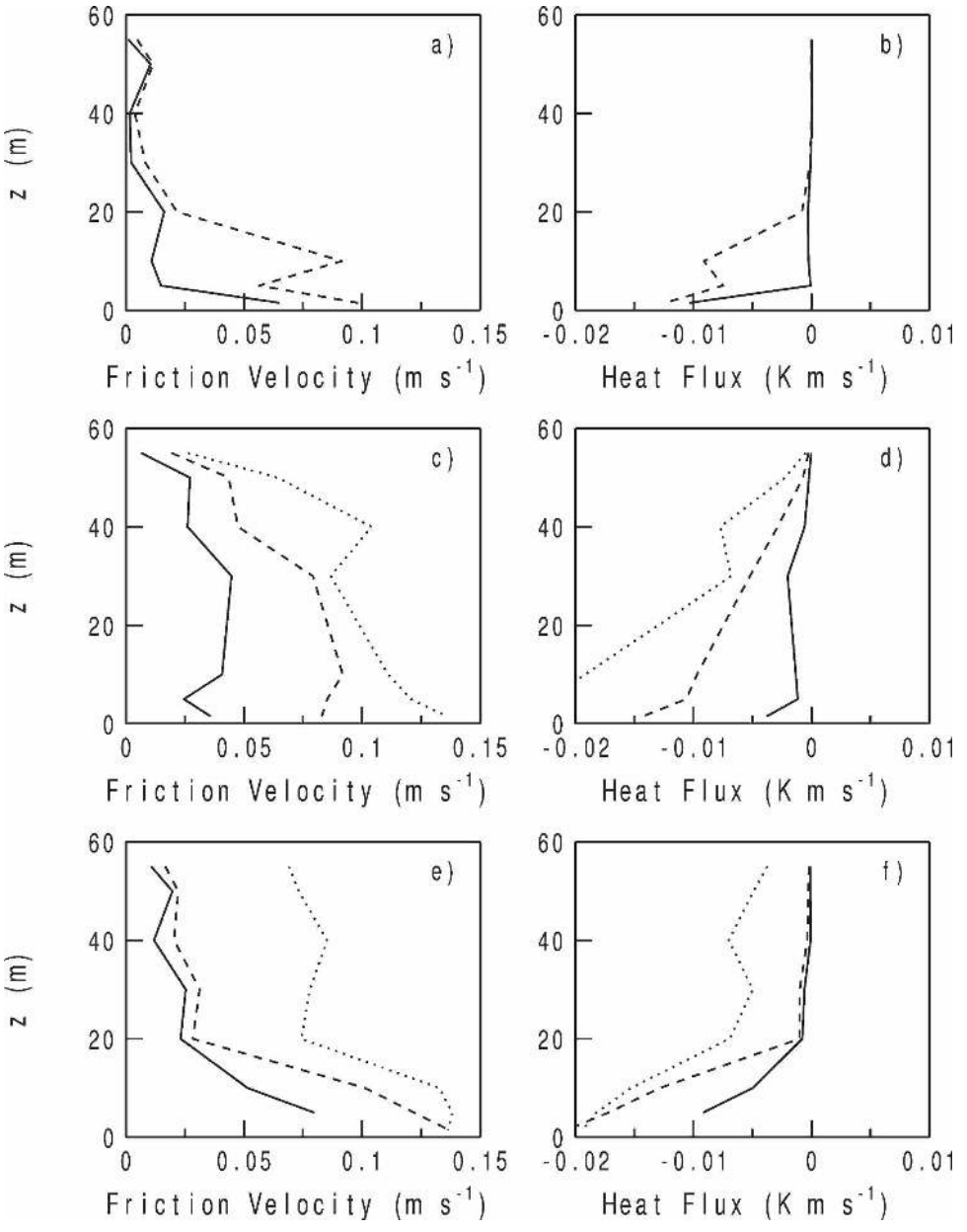

FIG. 10. Profiles with z of 60-min averaged u_* and H, showing traditional BL structure beneath quiescent layer for hours beginning 0400 and 0700 UTC (2200 and 0100 CST) (solid, dashed) on (a), (b) 18 Oct; for hours beginning 0200, 0300, and 0400 UTC (2000, 2100, and 2200 CST) (solid, dashed, dotted) on (c), (d) 6 Oct; and for hours beginning 0200, 0300, and 0400 UTC (2000, 2100, and 2200 CST) (solid, dashed, dotted) on (e), (f) 14 Oct.

(ii) 6 October

A somewhat stronger LLJ of 9 m s^{-1} for the night of 6 October (Fig. 4, fourth panel) produced stronger shear than on the previous three nights presented, and bulk Ri values between 0.2 and 0.3 (Ri_J was somewhat larger; Table 1). The most prominent feature on the time–height cross sections (e.g., Fig. 6d) was an elevated, isolated mixing event just before midnight local time (lasting from ~0520 to 0545 UTC), generated in the presence of the stronger shear. A second, much weaker mixing event occurred later at ~0900 UTC.

Prior to the events (Figs. 10c,d) the profiles exhibited weak fluxes compared with values observed on the strong LLJ nights in Table 1 (although somewhat stronger than on the three weaker-wind cases), and the

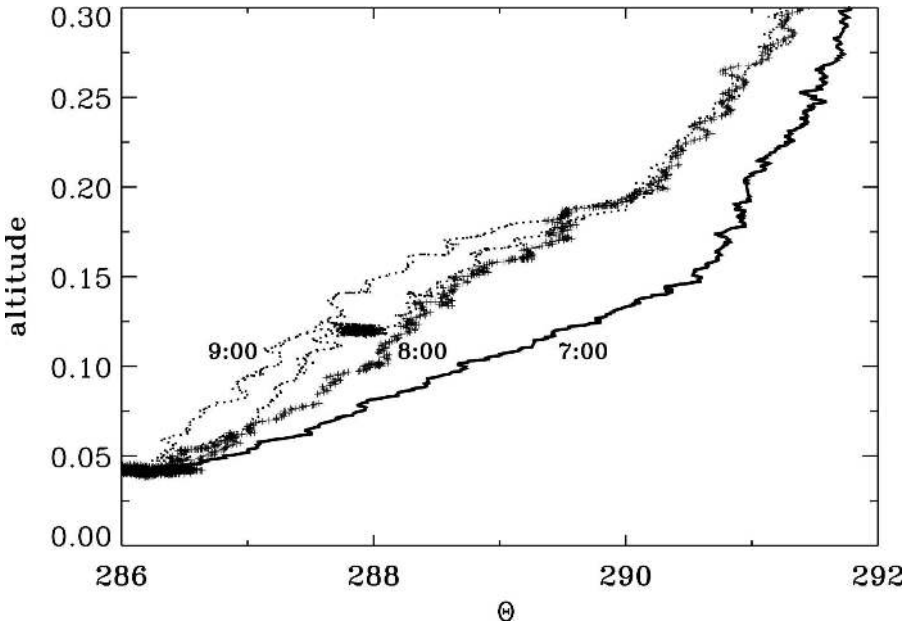

FIG. 11. Potential temperature soundings (K) for 14 Oct, showing strong stability in the subjet layer before 0800 UTC, and weaker stability afterward. Altitude is in kilometers above ground level and profiles are labeled in time UTC.

fluxes became negligibly small at 55 m, a higher level than on the other weak-wind nights. Thus, excluding the events, the structure of the SBL consisted of a weak, shear-driven boundary layer lying under a layer of negligible turbulent mixing, just as in the previous cases, but in somewhat stronger shear. The BL depth reached 55 m. In other words, despite a 9 m s^{-1} jet maximum at ~150 m above ground level (AGL) and interruption of the overall quiescent background turbulence state by the mixing events, the SBL between the events exhibited structure very similar to the previous cases, but with a higher BL top and somewhat stronger turbulence.

(iii) 14 October

Weak turbulence and mixing were observed at tower levels on this night in spite of a relatively stronger LLJ of 13 m s^{-1} at ~200-m height (Fig. 4) and relatively smaller values of $\mathrm{Ri_B}$ and $\mathrm{Ri_J}$. TLS profiles show that this was because of strong static stability in the layer below the jet nose (Fig. 11). Individual mixing events (Fig. 6e) can be seen at ~0400 UTC, as a result of a transient increase in wind speeds above 30 m and major increases in turbulence activity after 0800 UTC. Excluding these events, turbulence profiles show a shallow BL beneath a layer of negligible turbulent mixing (Figs. 10e,f), as in the previous cases. This is an example where effects other than the strength of the LLJ control turbulence intensity levels below the LLJ (Banta et al. 2006). In this case the surface was decoupled from LLJ-generated shear by a very stable θ profile for much of the night (Fig. 11), during which time the two-stratum structure was evident near the surface.

2) INTERRUPTIONS AND STRUCTURAL VARIATIONS

(i) 18 October

What distinguishes this night from the previous two very stable nights (26 and 20 October) were interruptions of the basic vSBL structure by three events—a density current at 0145 UTC (Sun et al. 2002), a solitary wave at 0630 UTC (Sun et al. 2004), and downward-propagating internal gravity waves during the early-morning hours at 1220 UTC (Sun et al. 2004), which have been analyzed in detail. The σ_w^2 cross section (Fig. 6c) indicates the first mixing event at 0200 UTC (which occurred during the evening transition) and the beginning of the third event at 1130 UTC (just before sunrise). The second event at about 0600 UTC was smoothed out of the cross section by the averaging. Sun et al. (2004) noted transient turbulence activity "adjacent to the ground" between events 2 and 3, which is reflected in Fig. 6c after 0800 UTC. These events are also seen in the u_* and H cross sections (not shown).

The turbulence profiles described in this section (Figs. 10a,b and 8c,d) were taken between the events and were not affected by them, except that a net down-

ward jump of <0.5°C accompanied the second event, indicating that this event did have a small, lingering vertical-transport effect on T at levels above the shallow BL. Except for this small effect the three events seemed to pass through the region, leaving the basic vSBL structure essentially unchanged. A Lagrangian interpretation could be that the disturbances had only a very localized effect on the SBL as they moved through the CASES array, and then they were replaced by undisturbed BL air that was never affected by the events. Thus, despite stronger shear and the interruption of the basic flow by mixing events, the vertical structure of the background turbulence between events was the same as the two-stratum structure of the two weak-wind cases.

(ii) 6 October

The two mixing events noted in Fig. 6d are evident in the cross sections for each of the turbulence variables, although only σ_w^2 is shown. The first event was a packet of shear-instability, Kelvin–Helmholtz-type waves, which has been investigated in detail by Newsom and Banta (2003), Blumen et al. (2001), and Poulos et al. (2002). As pointed out by Chimonas (1999), these patches of instability are likely to be of limited horizontal extent. Newsom and Banta (2003) calculated the length of this patch to be at least 6.75 km. The patch diameter is small compared with extents of more than 100 km, over which recent studies have reported Great Plains LLJs to have relatively uniform characteristics (Song et al. 2005; Banta et al. 2002). Therefore, despite comparatively vigorous mixing during the event, the effect on overall regionally averaged profiles was most likely much less than expected from the magnitude of the mixing within the patch (Chimonas 1999). Newsom and Banta (2003) show that after the passage of the event, the tower temperature traces became constant for at least an hour, suggesting a return to vSBL structure.

(iii) 14 October

On this night the two-stratum SBL structure was able to be maintained despite a relatively strong LLJ, because of strong stability in the subjet layer. But eventually, after 0800 UTC, the strong shear prevailed, and turbulence mixed downward through the tower layer (Fig. 6e), as the static stability decreased in this layer (Fig. 11). Balsley et al. (2006) have analyzed this period of strong mixing after 0800 UTC in detail, and attribute the increased depth of enhanced mixing to downward transport in a BL with upside-down structure (Mahrt 1999; Mahrt and Vickers 2002; Banta et al. 2002).

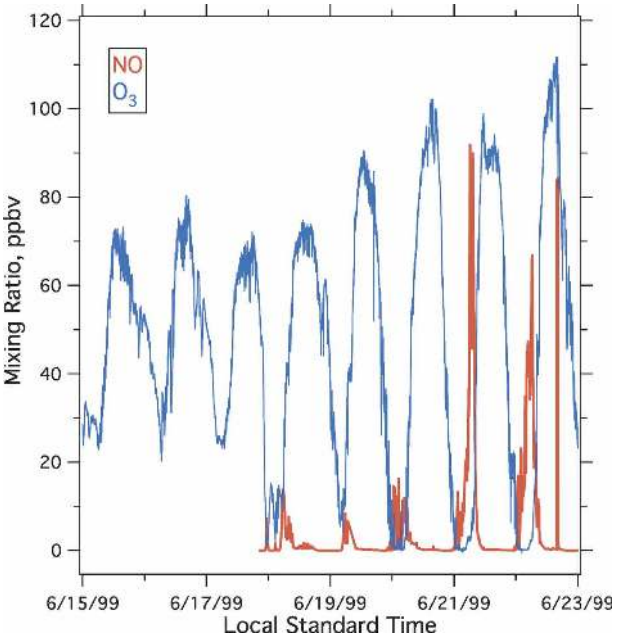

FIG. 12. Time series of ground-level ozone (blue line, 1-min values in ppb) at Cornelia Fort Airpark, Nashville, Tennessee, for 15–22 Jul 1999 (times UTC). Daytime hours are marked by the maxima in O_3 concentrations, and nights are the periods of minimum concentrations. NO measurements (red line, ppb) available after 17 Jun document local-source activity at this site at night. Late-night increases in NO concentrations on nights when the O_3 vanished indicate that the local emissions of NO were more than enough to titrate all the O_3.

4. Applications of vSBL structure

In this section we consider possible connections between SBL structure and near-surface ozone behavior, and some implications of the vSBL structure found in this study to the representation of surface mixing processes in NWP models.

a. Implications of vSBL structure to near-surface ozone concentrations

Here we consider how the kind of vSBL structure found in the previous section might help to understand the nighttime behavior of ground-level ozone (O_3). As a further advantage, we suggest that the behavior of O_3 may also aid in the interpretation of SBL turbulence measurements; O_3 is a trace species that is commonly measured because of its importance as an atmospheric pollutant. Figure 12 shows the diurnal behavior of ground-level concentrations of O_3 over several summertime days. This time series, which is typical of polluted land sites, was taken during the SOS-99 in Nashville, Tennessee, as part of a comprehensive set of high-quality air chemistry measurements (Thornton et al.

2003). Analyses presenting meteorological processes observed during the project are described in Darby et al. (2002) and White et al. (2003).

In this example, daytime values exceeding 70 parts per billion (ppb) were routinely much higher than nighttime values, because of higher pollutant emissions during the day and photochemical production. Although O_3 is produced during the daytime, above the BL at night it is mostly conserved, because the photochemical production is shut down and reactive losses are small away from emission source activity. Within the BL, removal processes (see appendix A), which include surface dry deposition and rapid chemical reactions with nitric-oxide (NO) emissions from near-surface combustion sources (including traffic), occur mostly near the surface.

On the earlier nights of Fig. 12 (e.g., 15–17 June), O_3 concentrations remained high, generally above 20 ppb. On the later nights of Fig. 13, however, O_3 concentrations vanished and remained at 0 for several hours (see, especially, 21–22 July). Doppler lidar profile data were available for some nights during SOS-99 (e.g., Darby et al. 2002; White et al. 2003). On nights when the lidar data indicated stronger speeds (7–8 m s^{-1} or more), higher O_3 concentrations lasted throughout the night. But nights when the lidar-measured weak LLJ speeds (peaks of 3–4 m s^{-1} or less below 200 m AGL) were nights when the ground-level O_3 vanished.

The former behavior shows the effects of vertical mixing or transport. On the stronger-LLJ (stronger-wind) nights, enhanced vertical mixing would bring down fresh O_3 (e.g., Corsmeier et al. 1997; Reitebuch et al. 2000; Nappo 1991; Darby et al. 2002) and would distribute the effects of O_3 removal over the deeper layer (Fig. 13, right), resulting in persistence of relatively higher ground-level concentrations. This behavior would be expected in a BL, in which some significant level of vertical mixing—either by turbulent diffusion or other processes—was always present. Under stronger wind conditions Banta et al. (2006) have argued that the top of the SBL (corresponding to the height of the LLJ nose) may not act as a lid; that is, quantities may leak upward or downward through this level.

On the other hand, O_3 concentrations became zero at the surface on the weak-wind, very stable nights. An issue is how the O_3 could disappear if some background level of vertical mixing or transport were present. The disappearance could be explained by horizontal advection of clean air or advection of high concentrations of local emissions. These explanations seem unlikely, though, because 1) the winds were light on these nights, minimizing advective distances, 2) O_3 disappeared on each light-wind night, even though mean wind directions varied (emission-source activity would appear strongest from preferred directions), 3) the buildup of NO on nights when $O_3 \rightarrow 0$ indicated limited mixing, and 4) the presence of other pollutants indicated that the depeleted-O_3 air was from a polluted air mass.

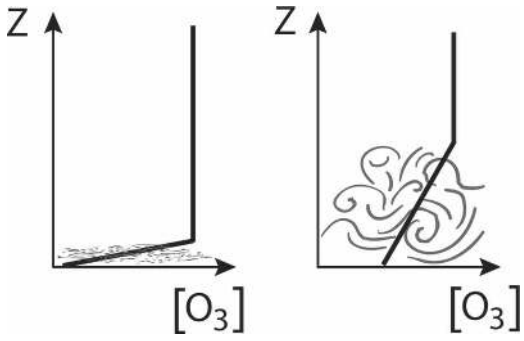

FIG. 13. Schematic representation of ozone distribution with (left) height for the vSBL and (right) the stronger-wind SBL.

An alternative explanation is that vertical exchange vanished at some level not far above the surface (Fig. 13, left). This explanation would be consistent with the two-stratum structure found in section 3, with the quiescent layer acting as a lid, trapping the O_3 in the shallow BL along with the NO emissions. Removal processes would be able to deplete this very shallow layer of O_3. The existence of this structure, which we have associated with very stable conditions, is a result of light winds and weak shears producing large Ri_B and Ri_J. In the moist Tennessee environment, inversions and $\partial\theta/\partial z$ would be expected to be weaker than in Kansas, but the relevant measure of stability, Ri_B, was still large, because of the small shear values, which appear squared in the denominator of Ri_B.

The O_3 data are presented to illustrate the kind of supplementary information that can be provided by trace-species measurements. It is suggested that the ozone disappearance for several hours during the night could be diagnostic of the very stable, two-stratum structure. If true, the fact that this kind of O_3 disappearance is widely observed in many different geographic regions would imply that the occurrence of the kind of vSBL structure described here is also widespread. But at this point the relationship must be regarded as tentative, because, as has been true for most field programs, sophisticated turbulence measurements were not available for SOS and high-quality air chemistry (including O_3) measurements were not taken during CASES-99. It seems evident that careful trace-species measurements could add significant supplementary information on the effects of vertical mixing (or the lack of such mixing), which could be critical to the cor-

rect interpretation of a dataset. Especially powerful would be to have such species measurements at multiple vertical levels. A number of tracers have been used. For example, mixing properties have been inferred in the nighttime SBL from chemical species such as O_3, radon, and carbon dioxide (e.g., Corsmeier et al. 1997; Reitebuch et al. 2000; Darby et al. 2002; Banta et al. 1997, 1998; Salmond and McKendry 2002; Salmond 2005; Kataoka et al. 2001, 2003; Karipot et al. 2006; Mathieu et al. 2005).

b. NWP surface-layer applications

Time series of T at the upper tower levels (40–55 m) and an O_3 time series example support the idea that that turbulence was strongly inhibited in a layer just above the shallow BL in strongly stable conditions. The finding that surface properties were not being mixed upward into the atmosphere (Fig. 14) was based on the CASES-99 instrument array. If this finding proved to be of general applicability, it is worth considering the implications of such a layer of ineffective vertical transport to the parameterization of the vSBL in NWP models. This quiescent layer would essentially detach the bulk of the modeled atmosphere from the surface. As related to atmospheric nocturnal budgets and the parameterization of the surface layer in NWP models, it would act as an essentially dead layer between the surface and the bulk of the atmosphere above the shallow BL. The absence of interaction between the earth's surface and the atmosphere above the shallow BL suggests that an appropriate lower boundary condition for the model under such conditions may be a free-slip, thermally insulated layer, in which no exchange of trace species between the atmospheric (predictive) model and the surface or the shallow BL below would be permitted. In other words, the surface-layer parameterization, expressing transfer through the surface layer and into the model, should allow the fluxes to become vanishingly small [the sharp-tails dependence on stability of Beare et al. (2006)] or even zero, when in the very stable Ri_J or Ri_B regime. We note that this is probably the simplest lower boundary condition, and as such, it would seem worthwhile at least to test this approach.

What would be the advantages over current numerical schemes? One of the basic problems in current models is that the residual diffusion inherent in the numerics and the required minimum specified levels of turbulence or eddy diffusivities, which are needed to maintain numerical stability, can introduce excessive fictitious, nonphysical mixing. If the surface and the surface layer were at all connected to (numerically in communication with, so to speak) the lowest predictive grid points of the simulated atmosphere, surface properties will artificially propagate upward into the model atmosphere, regardless of static stability. It is hypothesized here that suppressing this diffusion into the model is more physically realistic than allowing the lowest predictive model grid point to interact with the surface, although we acknowledge that with current model tuning, models may not be able to accommodate such decoupling from the surface (e.g., removal of momentum by surface friction or thermal-budget effects leading to runaway cooling) without further alteration of other modeled processes. These issues have previously been considered by Derbyshire (1999) and Mahrt (1998).

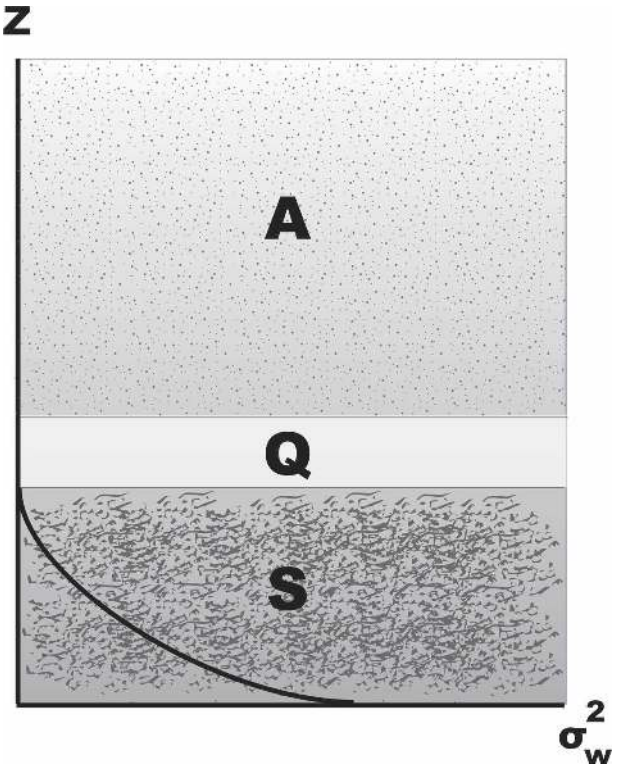

FIG. 14. Schematic representation of shallow BL (S), quiescent layer (Q), and atmosphere above quiescent layer (A), showing the vertical relationship between the two lowest atmospheric layers (S and Q) and the atmosphere above (A). The region A (which may include the remnants of the previous afternoon's mixed layer and the free atmosphere) is not addressed in this study, but most likely consists of many layers itself, at least some having intermittent turbulence. The important issue for this study is whether atmospheric properties at the surface or in S are transported by any means up into region A.

Lower bounds (or long-tails stability dependence; Beare et al. 2006) for surface fluxes, especially the heat flux, prevent the runaway effects. Recently, however, some of the other modeled processes in the surface energy budget have been shown to have problems, such as radiation and surface energy budget (Zhong and Fast

2003; Zamora et al. 2003) and the fluxes into the ground (Van de Wiel et al. 2003; Van de Wiel 2006, personal communication; Steeneveld et al. 2007; Banta and Gannon 1995). Improving representation of these other processes may be sufficient to prevent the runaway effects, and thus avoid the need to keep turbulent fluxes unrealistically high.

5. Conclusions

The focus of this study has been on the impacts of a layer of strongly suppressed mixing on surface–atmosphere turbulent transport. The layer sat just above the traditional BL in light-wind, cloud-free, very stable conditions. The BL under these conditions was found to be very shallow (sometimes less than 10 m deep) in agreement with two previous studies. The extreme weakness of the turbulence above the shallow BL became apparent after application of an analysis procedure that effectively filters out low-frequency disturbances to reveal the contribution of exclusively turbulent processes to vertical exchange. The weak turbulence aloft was also evident in tethered lifting system profiles of TKE dissipation.

Very stable conditions were defined with respect to large bulk Richardson number Ri_B (or Ri_J), primarily resulting from small values of shear in the weak-wind BL. Although the winds were light, the wind profile was found to exhibit periods of an hour or so, when the shape and magnitude of the profile changed little. At times this persistent profile could achieve a weak jetlike shape, but sometimes no such maximum was evident—just weak winds below 200 m.

The implications of this two-layer or two-stratum structure—the shallow BL next to the ground and the quiescent layer (QL) just above—is that the atmosphere above the shallow BL is completely decoupled and isolated from surface effects (Fig. 14). Evidence from temperature time series and from the disappearance of ground-level ozone at night imply that near-surface properties were not being mixed upward to levels above the shallow BL, and conversely, properties above the shallow BL were not being mixed downward into the BL. This contrasts with nights with intermediate or strong LLJs, where shear generation of turbulence below the jet becomes coupled with the surface layer.

These findings were from data analyses for the two weakest LLJ nights of CASES-99. The SBLs on other nights when LLJ speeds were modestly stronger also exhibited the two-stratum structure with a shallow BL next to the surface, but they also showed an increased incidence of traveling mesoscale disturbances. Available data from the dataset analyzed here indicated that such disturbances could pass through a region, leaving the basic structure of the SBL more or less unaffected. Based on this observation, appendix B suggests several testable hypotheses for future research efforts, in which the effect of these disturbances on the evolution of areawide mean vertical profiles is initially viewed as being negligible.

The two-stratum structure, which we found typical of vSBLs, was also found on a night with an even stronger LLJ (13 m s^{-1}), when the shear generated by the LLJ was isolated from the BL by strong stability in the layer below the LLJ nose. Eventually LLJ-generated turbulence burst downward to the surface to couple LLJ turbulence aloft to the surface, but for a period of 6 h, vSBL structure was observed near the surface despite the stronger LLJ.

An open issue that requires further investigation is the depth of the quiescent layer aloft. The possibilities are that the layer is of limited depth with more turbulence above, or that once the turbulence and mixing become negligible at the top of the shallow BL, they remain so up through the troposphere. Some data seem to indicate that turbulence exists above the QL, acting as an upper bound to this layer as may be suggested in Fig. 14 (cf. Figs. 8a,b, 7a), whereas other profiles show no increases in turbulence above the shallow BL (cf. Figs. 8c,d and other profiles in Figs. 7 and 10), as suggested by Fig. 1 extended vertically. Finding both types of turbulence structure in this region aloft may reflect the sporadic, intermittent nature of turbulence in the region. In either case, the conclusions of this study are unaffected, since both structures would permit no mixing just above the shallow BL, and both would result in a disconnect between the surface and the atmosphere above the BL.

The suppression of exchange between the surface and the atmosphere by the QL might seem to imply that processes within the shallow BL are largely irrelevant to the atmosphere as a whole, for example to NWP applications. However, the near-surface layer is of great practical importance for forecasting, as this is the layer occupied by most human activity. Overnight minimum temperatures, fog formation, and mass budgets of airborne contaminants and their ground-level concentrations are a few of the critical forecasting challenges, and so it will be necessary to consider how a model should handle the shallow BL. From the preceding discussion, this layer would need to be treated as an entity isolated from the rest of the model, perhaps even diagnostically. The practical importance of the shallow BL warrants continued study of its properties.

Acknowledgments. This study began as a weeklong meeting between the NOAA and Oregon State University groups in Corvallis during June 2004, funded by the U.S. Army Research Office (ARO, Dr. Walter Bach) of the Army Research Laboratory under Proposal 43711-EV and Grant DAAD19-0210224. Ozone and air-chemistry analysis was supported by the NOAA Health of the Atmosphere program. This study is based upon work supported by ARO under Grant DAAD19-0210224 (OSU), Proposal 43711-EV (NOAA), and Contracts DAAD-19-99-1-0320 (JS, NCAR), and DAAD-19-02-1-0435 (BBB, CIRES); and Grants 0107617-ATM (LM and DV, OSU), ATM-9906637 (JS, NCAR), and ATM-0128-089 (BBB, CIRES) from the Physical Meteorology Program of the National Science Foundation (NSF). Funding for the CASES-99 HRDL field measurements was provided by the Army Research Office under Proposal 40065-EV, the Cooperative Institute for Research in the Atmosphere (Center for Geosciences/Atmospheric Research) at Colorado State University, and NSF Grant ATM-9908453 (HRDL). Further analysis and manuscript preparation for this research were supported by the Office of Science (BER), U.S. Department of Energy, under Interagency Agreement DE-AI02-04ER63860 (VTMX). We appreciate important contributions to this research by Dr. R. K. Newsom and to the manuscript and figure preparation by Ms. Lisa Darby, and helpful reviews of the manuscript provided by Ms. Darby, and Drs. Andrei Grachev and Ola Persson.

APPENDIX A

Nighttime Ozone Removal

Nighttime ozone removal can occur by two distinct processes. The first is via dry deposition, a permanent, irreversible loss to vegetation and other surfaces. Deposition removes a fraction of the existing concentration, so it is not likely to completely remove a substance from the air mass. The second is via rapid chemical reaction or titration, principally involving nitrogen-oxide (NO, NO_2) emissions (if no local emissions were present, some removal could also be effected by other, slower chemical reactions). Emissions of NO, which can come from traffic or other local near-surface combustion activities at night, converts O_3 to NO_2 plus oxygen molecules on a time scale of seconds. But the next morning, photochemical processes convert the enhanced NO_2 concentrations back to elevated O_3 concentrations, so this process does not represent a permanent loss of O_3 to the atmosphere.

As described in the text, on the very stable nights when winds and vertical mixing were weak, the local emissions would be trapped within the shallow BL, where they would remain at high concentrations and could titrate all the O_3, driving O_3 concentrations in the shallow BL to 0 (given sufficient NO). On the other hand, when the winds and vertical mixing were stronger, the emissions would be diluted over a much deeper layer, reducing titration effects on O_3 concentrations, and fresh O_3 would also continually be brought down to the surface. The effect would be to keep ground-level O_3 concentrations higher, as summarized in Fig. 13.

When considering the buildup of O_3 pollution over several days of a pollution episode, it is necessary to consider how much total O_3 could be lost during nighttime hours. This implies consideration of the effects of nighttime removal processes on the column O_3 budget. In the light-wind, very stable case, the total amount of O_3 exposed to surface removal processes would be confined to the shallow BL, because of the lack of vertical mixing out of the shallow BL and up into the quiescent layer, as described. In other words, the shallow BL would be the only portion of the atmosphere interacting with the ground, as far as O_3 was concerned (Fig. 13, left). Thus, considering a vertical column of O_3 a kilometer or so deep (i.e., deep enough to include the previous afternoon mixed-layer depth), the total amount of O_3 lost via surface deposition would be insignificant. This would be true even if all the O_3 in the shallow BL were lost to the surface, but, of course, a significant fraction of it would have been titrated and therefore not irreversibly lost. In the strong-wind case the continual replenishment of O_3 at the surface would mean greater exposure of O_3 to the surface from a deeper layer and thus greater removal rates via deposition, representing a permanent loss of O_3 to the atmosphere (Fig. 13, right). Interestingly, effects similar to these have been noted in mountainous terrain flows by Broder and Gygax (1985) and Banta et al. (1997). Thus, it is perhaps ironic that on the nights when surface O_3 remained high, total O_3 losses through a vertical column would be greater, whereas on nights when surface O_3 concentrations became zero, losses through the column would be minimal, because dry-deposition losses would occur only from a very thin layer. Viewed in this way, on the weak-LLJ nights when the O_3 vanished, the O_3 time series data indicate a nearly complete disconnect between the shallow, surface-based BL and the atmosphere higher up.

APPENDIX B

Future Measurement Studies

On several of the nights considered, the overall quiescence of the SBL and above was interrupted by tur-

bulence events, such as shear instabilities and density currents. An important question for understanding the vSBL is: what is the impact of these events on vertical mixing and on the evolution of the vertical structure of the SBL? Do these events perform a significant amount of mixing and affect the near-surface, area-wide profiles of momentum, temperature, etc. In other words, is it the inhomogeneities—the periods thrown out of traditional analyses—that do most of the mixing? Or, do these events have only transient localized effects and pass through, leaving the profiles averaged over a wide area largely unchanged? Case studies presented in this paper have suggested that often the effects of these disturbances have limited extent, and that the SBL may remain relatively unchanged after they have passed through. These important questions should be the focus of future field research.

Several hypotheses, which may be useful to consider when designing future field programs, have been suggested by this research, including: When the maximum wind speeds in the lowest 200 m are less than 10 m s^{-1} under very stable conditions, such as clear nights over land:

- A shallow BL forms, and the effective height scale of the very stable boundary layer for most applications is the 10–30-m depth of the shallow BL.
- No effective exchange by turbulent mixing processes exists between the surface and the atmosphere above the shallow BL.
- Turbulent events act only as interruptions of the quiescent BL and have little net effect on area-averaged BL vertical profiles or structure—overall vertical mixing effects of these events is negligible.
- The vSBL can be modeled as a free slip, thermally insulated lower boundary with no source or sink activity with respect to the atmospheric model.
- Localized regions of w from topographically induced horizontal convergence/divergence patterns have no effect on vertical transport between the surface and the atmosphere above the shallow BL.

We note that the 10 m s^{-1} criterion may vary from region to region; for example regions where radiative cooling is not so strong may produce weaker static stability and more turbulent mixing at lower LLJ wind speeds. Research may confirm that a bulk Ri is the appropriate indicator of very stable conditions.

REFERENCES

Acevedo, O. C., O. L. L. Moraes, G. A. Degrazia, and L. E. Medeiros, 2006: Intermittency and the exchange of scalars in the nocturnal surface layer. *Bound.-Layer Meteor.,* **119,** 41–55.

Baas, P., G. J. Steeneveld, B. J. H. van de Wiel, and A. A. M. Holtslag, 2006: Exploring self-correlation in the flux–gradient relationships for stable stratified conditions. *J. Atmos. Sci.,* **63,** 3045–3054.

Balsley, B. B., M. L. Jensen, and R. G. Frehlich, 1998: The use of state-of-the-art kites for profiling the lower atmosphere. *Bound.-Layer Meteor.,* **87,** 1–24.

——, R. G. Frehlich, M. L. Jensen, Y. Meillier, and A. Muschinski, 2003: Extreme gradients in the nocturnal boundary layer: Structure, evolution, and potential causes. *J. Atmos. Sci.,* **60,** 2496–2508.

——, ——, ——, and ——, 2006: High-resolution in situ profiling through the stable boundary layer: Examination of the SBL top in terms of minimum shear, maximum stratification, and turbulence decrease. *J. Atmos. Sci.,* **63,** 1291–1307.

Banta, R. M., and P. T. Gannon, 1995: Influence of soil moisture on simulations of katabatic flow. *Theor. Appl. Climatol.,* **52,** 85–94.

——, and Coauthors, 1997: Nocturnal cleansing flows in a tributary valley. *Atmos. Environ.,* **31,** 2147–2162.

——, and Coauthors, 1998: Daytime buildup and nighttime transport of urban ozone in the boundary layer during a stagnation episode. *J. Geophys. Res.,* **103,** 22 519–22 544.

——, R. K. Newsom, J. K. Lundquist, Y. L. Pichugina, R. L. Coulter, and L. Mahrt, 2002: Nocturnal low-level jet characteristics over Kansas during CASES-99. *Bound.-Layer Meteor.,* **105,** 221–252.

——, Y. L. Pichugina, and R. K. Newsom, 2003: Relationship between low-level jet properties and turbulence kinetic energy in the nocturnal stable boundary layer. *J. Atmos. Sci.,* **60,** 2549–2555.

——, ——, and W. A. Brewer, 2006: Turbulent velocity-variance profiles in the stable boundary layer generated by a nocturnal low-level jet. *J. Atmos. Sci.,* **63,** 2700–2719.

Beare, R. J., and Coauthors, 2006: An intercomparison of large-eddy simulations of the stable boundary layer. *Bound.-Layer Meteor.,* **118,** 247–272.

Blumen, W., R. M. Banta, S. P. Burns, D. C. Fritts, R. K. Newsom, G. S. Poulos, and J. Sun, 2001: Turbulence statistics of a Kelvin-Helmholtz billow event observed in the nighttime boundary layer during the CASES-99 field program. *Dyn. Atmos. Oceans,* **34,** 189–204.

Broder, B., and H. A. Gygax, 1985: The influence of locally induced wind systems on the effectiveness of nocturnal dry deposition of ozone. *Atmos. Environ.,* **19,** 1627–1637.

Burns, S. P., and J. Sun, 2000: Thermocouple temperature measurements from the CASES-99 main tower. Preprints, *14th Symp. on Boundary Layers and Turbulence,* Snowmass, CO, Amer. Meteor. Soc., 358–361.

Chimonas, G., 1999: Steps, waves, and turbulence in the stably stratified planetary boundary layer. *Bound.-Layer Meteor.,* **90,** 397–421.

Corsmeier, U., N. Kalthoff, O. Kolle, M. Kotzian, and F. Fiedler, 1997: Ozone concentration jump in the stable nocturnal boundary layer during a LLJ event. *Atmos. Environ.,* **31,** 1977–1989.

Darby, L. S., and Coauthors, 2002: Vertical variations in O_3 concentrations before and after a gust front passage. *J. Geophys. Res.,* **107D,** 4321, doi:10.1029/2001JD000996.

Derbyshire, S., 1999: Boundary-layer decoupling over cold surfaces as a physical boundary-instability. *Bound.-Layer Meteor.,* **90,** 297–325.

Frehlich, R. G., Y. Meillier, M. L. Jensen, and B. B. Balsley, 2003: Turbulence measurements with the CIRES Tethered Lifting

System during CASES-99: Calibration and spectral analysis of temperature and velocity. *J. Atmos. Sci.,* **60,** 2487–2495.

Grachev, A., C. W. Fairall, P. O. G. Persson, E. L Andreas, and P. S. Guest, 2005: Stable boundary layer scaling regimes: The SHEBA data. *Bound.-Layer Meteor.,* **116,** 201–235.

Grund, C. J., R. M. Banta, J. L. George, J. N. Howell, M. J. Post, R. A. Richter, and A. M. Weickmann, 2001: High-resolution Doppler lidar for boundary-layer and cloud research. *J. Atmos. Oceanic Technol.,* **18,** 376–393.

Holtslag, A. A. M., and F. T. M. Nieuwstadt, 1986: Scaling in the atmospheric boundary layer. *Bound.-Layer Meteor.,* **36,** 201–209.

——, and H. A. R. De Bruin, 1988: Applied modeling of nighttime surface energy balance over land. *J. Appl. Meteor.,* **27,** 689–704.

Karipot, A., M. Y. Leclerc, G. Zhang, T. Martin, G. Starr, D. Hollinger, J. H. McCaughey, and G. R. Hendrey, 2006: Nocturnal CO_2 exchange over a tall forest canopy associated with intermittent low-level jet activity. *Theor. Appl. Climatol.,* **85,** 243–248.

Kataoka, T., and Coauthors, 2001: A study of the atmospheric boundary layer using radon and air pollutants as tracers. *Bound.-Layer Meteor.,* **101,** 131–155.

——, and Coauthors, 2003: Concentrations of ^{222}Rn, its short-lived daughters, and ^{212}Pb and their ratios under complex atmospheric concentrations and topography. *Bound.-Layer Meteor.,* **107,** 219–249.

Klipp, C. L., and L. Mahrt, 2004: Flux-gradient relationship, self-correlation and intermittency in the stable boundary layer. *Quart. J. Roy. Meteor. Soc.,* **130,** 2087–2103.

Louis, J.-F., 1979: A parametric model of vertical eddy fluxes in the atmosphere. *Bound.-Layer Meteor.,* **17,** 187–202.

Mahrt, L., 1985: Vertical structure and turbulence in the very stable boundary layer. *J. Atmos. Sci.,* **42,** 2333–2349.

——, 1998: Stratified atmospheric boundary layers and breakdown of models. *J. Theor. Comp. Fluid Dyn.,* **11,** 263–280.

——, 1999: Stratified atmospheric boundary layers. *Bound.-Layer Meteor.,* **90,** 375–396.

——, and D. Vickers, 2002: Contrasting vertical structures of nocturnal boundary layers. *Bound.-Layer Meteor.,* **105,** 351–363.

——, and ——, 2006: Extremely weak mixing in stable conditions. *Bound.-Layer Meteor.,* **119,** 19–39.

——, J. Sun, W. Blumen, T. Delaney, and S. Oncley, 1998: Nocturnal boundary layer regimes. *Bound.-Layer Meteor.,* **88,** 255–278.

——, D. Vickers, R. Nakamura, M. R. Soler, J. Sun, S. P. Burns, and D. H. Lenschow, 2001: Shallow drainage flows. *Bound.-Layer Meteor.,* **101,** 243–260.

Mathieu, N., I. B. Strachan, M. Y. LeClerc, A. Karipot, and E. Pattey, 2005: Role of low-level jets and boundary-layer properties on the NBL budget technique. *Agric. For. Meteor.,* **135,** 35–43.

Muschinski, A., R. G. Frehlich, and B. B. Balsley, 2004: Small-scale and large-scale intermittency in the nocturnal boundary layer. *J. Fluid Mech.,* **515,** 319–351.

Nappo, C. J., 1991: Sporadic breakdowns of stability in the PBL over simple and complex terrain. *Bound.-Layer Meteor.,* **54,** 69–87.

Newsom, R. K., and R. M. Banta, 2003: Shear-flow instability in the stable nocturnal boundary layer as observed by Doppler lidar during CASES-99. *J. Atmos. Sci.,* **30,** 16–33.

Ohya, Y., 2001: Wind-tunnel study of atmospheric stable boundary layers over a rough surface. *Bound.-Layer Meteor.,* **98,** 57–82.

Poulos, G. S., and S. P. Burns, 2003: An evaluation of bulk Ri-based surface layer flux formulas for stable and very stable conditions with intermittent turbulence. *J. Atmos. Sci.,* **60,** 2523–2537.

——, and Coauthors, 2002: CASES-99: A comprehensive investigation of the stable nocturnal boundary layer. *Bull. Amer. Meteor. Soc.,* **83,** 555–581.

Reitebuch, O., A. Strassburger, S. Emeis, and W. Kuttler, 2000: Nocturnal secondary ozone concentration maxima analysed by sodar observations and surface measurements. *Atmos. Environ.,* **34,** 4315–4329.

Salmond, J. A., 2005: Wavelet analysis of intermittent turbulence in a very stable nocturnal boundary layer: Implications for the vertical mixing of ozone. *Bound.-Layer Meteor.,* **114,** 463–488.

——, and I. G. McKendry, 2002: Secondary ozone maxima in a very stable nocturnal boundary layer: Observations from the Lower Fraser Valley. *Atmos. Environ.,* **36,** 5771–5782.

Smedman, A.-S., 1988: Observations of a multi-level turbulence structure in a very stable atmospheric boundary layer. *Bound.-Layer Meteor.,* **44,** 231–253.

Soler, M. R., C. Infante, P. Buenestado, and L. J. Mahrt, 2002: Observations of nocturnal drainage flows in a shallow gully. *Bound.-Layer Meteor.,* **105,** 253–273.

Song, J., K. Liao, R. L. Coulter, and B. M. Lesht, 2005: Climatology of the low-level jet at the Southern Great Plains Atmospheric Boundary Layer Experiments site. *J. Appl. Meteor.,* **44,** 1593–1606.

Steeneveld, G.-J., B. J. H. van de Wiel, and A. A. M. Holtslag, 2007: Diagnostic equations for the stable boundary layer height: Evaluation and dimensional analysis. *J. Appl. Meteor.,* **46,** 212–225.

Sun, J., and Coauthors, 2002: Intermittent turbulence associated with a density current passage in the stable boundary layer. *Bound.-Layer Meteor.,* **105,** 199–219.

——, S. P. Burns, A. C. Delaney, S. P. Oncley, T. W. Horst, and D. H. Lenschow, 2003: Heat balance in the nocturnal boundary layer during CASES-99. *J. Appl. Meteor.,* **42,** 1649–1666.

——, and Coauthors, 2004: Intermittent turbulence in stable boundary layers and the processes that generate it. *Bound.-Layer Meteor.,* **110,** 255–279.

Thornton, J. A., P. J. Wooldridge, R. C. Cohen, E. J. Williams, D. Hereid, F. C. Fehsenfeld, J. Stutz, and B. Alicke, 2003: Comparison of in situ and long path measurements of NO2 in urban plumes. *J. Geophys. Res.,* **108,** 4496, doi:10.1029/2003JD003559.

Van den Kroonenberg, A., and J. Bange, 2007: Turbulent flux calculation in the polar stable boundary layer: Multiresolution flux decomposition and wavelet analysis. *J. Geophys. Res.*, **112,** D06112, doi:10.1029/2006JD007819.

Van de Wiel, B. J. H., A. F. Moene, R. J. Ronda, H. A. R. De Bruin, and A. A. M. Holtslag, 2002: Intermittent turbulence in the stable boundary layer over land. Part II: A system dynamics approach. *J. Atmos. Sci.,* **59,** 2567–2581.

——, ——, O. Hartogensis, H. A. R. De Bruin, and A. A. M. Holtslag, 2003: Intermittent turbulence in the stable boundary layer over land. Part III: A classification for observations during CASES-99. *J. Atmos. Sci.,* **60,** 2509–2522.

Vickers, D., and L. Mahrt, 1997: Quality control and flux sampling

problems for tower and aircraft data. *J. Atmos. Oceanic Technol.,* **14,** 512–526.

——, and ——, 2003: The cospectral gap and turbulent flux calculations. *J. Atmos. Oceanic Technol.,* **20,** 660–672.

——, and ——, 2006: A solution for flux contamination by mesoscale motions with very weak turbulence. *Bound.-Layer Meteor.,* **118,** 431–447.

White, A. B., and Coauthors, 2003: Regional contrast in the morning transitions observed during the 1999 Southern Oxidants Study Nashville/middle Tennessee intensive. *J. Geophys. Res.,* **107,** 4726, doi:10.1029/2001JD002036.

Wulfmeyer, V. O., M. Randall, W. A. Brewer, and R. M. Hardesty, 2000: 2 μm Doppler lidar transmitter with high frequency stability and low chirp. *Opt. Lett.,* **25,** 1228–1230.

Zamora, R. J., and Coauthors, 2003: Comparing MM5 radiative fluxes with observations gathered during the 1995 and 1999 Nashville Southern Oxidants Study. *J. Geophys. Res.,* **108,** 4050, doi:10.1029/2002JD002122.

Zhong, S., and J. D. Fast, 2003: An evaluation of the MM5, RAMS, and Meso-Eta models at subkilometer resolution using field campaign data in the Salt Lake Valley. *Mon. Wea. Rev.,* **131,** 1301–1322.

Zilitinkevich, S., 1972: On the determination of the height on the Ekman boundary layer. *Bound.-Layer Meteor.,* **3,** 141–145.